

www.acsanm.org Article

Engineering Viscoelasticity in Autoregulatory Nanoscale Wrinkling Bilayer Hydrogel Systems: Pressure Sensors and Thermal-Responsive Drug Delivery Systems

Zeynab Mousavikhamene and George C. Schatz*





ACCESS

Metrics & More

Article Recommendations

Supporting Information

soft substrate

heating

incident light
scattered light
absorbed light

ABSTRACT: This paper explains the wrinkling behavior of a bilayer system comprised of a soft, thick hydrogel on a hard thin skin in which the hydrogel has viscoelastic properties. The role of external stress and viscoelastic properties on the morphology of nanoscale wrinkles is discussed in a time-dependent mechanical and thermomechanical framework and compared with the corresponding results from a linear elastic treatment of the hydrogel. Our results show that the strain rate and magnitude of strain have substantial impact on nanoscale wrinkle morphology when viscoelasticity of the substrate is included in the model. As such, engineering the relaxation time through the material synthesis process or material selection plays an important role. This is important to modeling an autoregulatory humidity sensing device that was previously developed by our group and others, where the formation of humidity-dependent nanoscale wrinkles tunes the transmission or scattering of light through the substrate, thereby enabling a plasmonic nanoparticle array to switch on or off plasmonic heating of the system that generates or removes the nanoscale wrinkles. Three different lumped viscoelastic models are applied: generalized Maxwell (GM), generalized Kelvin-Voigt (GK), and Burger (BR) models. Time evolution analysis of these models, including comparison with the validated linear elastic model at high relaxation time and with experimental data, shows best agreement with the GK result. Finally, we quantitatively demonstrate how the morphology of nanoscale wrinkles that is accessible to viscoelastic models can adjust the light transmission across the substrate by amounts that are useful for the autoregulatory device. This viscoelastic modeling will enable more quantitative predictions and design principles for taking advantage of responsive materials such as for pressure or humidity sensors or thermal-responsive drug delivery systems.

KEYWORDS: viscoelastic, wrinkling, hydrogel, autoregulatory, bilayer material

■ INTRODUCTION

A layered composite system consisting of a hard thin skin on a soft, thick substrate undergoes nanoscale to microscale wrinkling when the system is under compression with a sufficient magnitude. The wrinkling of layered systems requires having bilayered materials (e.g., elastomers as substrate and Teflon as skin) with substantially different mechanical (Young's modulus) properties. Wrinkling occurs when sufficient strain is applied to one of the layers, as wrinkling reduces the internal stress. Wrinkle formation due to mechanical instabilities is widely used, with applications to tunable temporal autoregulatory systems, ¹ flexible elec-

tronics,^{2,3} cell growth controlling substrates,^{4,5} microcontact printing stamps, photolithography masks,^{6,7} pressure sensors,⁸ and chemical sensors.⁹ In general, the nanoscale or microscale surface patterns that result from wrinkling enable control of optical (e.g., scattering and transmitting of light^{1,10,11}),

Received: August 3, 2022 Accepted: August 8, 2022 Published: August 23, 2022





chemical (e.g., hydrophobicity^{12–14}), and physical (e.g., roughness^{15,16}) properties of layered surfaces. Hence, predicting and controlling the pattern of nanoscale wrinkles such as their wavelength and amplitude is of utmost importance. This can be manipulated by different parameters such as magnitude of strain, Young's modulus and Poisson's ratio of substrate to that of skin, and skin thickness.

There have been several mechanical wrinkling systems studied experimentally using thermal or mechanical perturbations. ^{17–26} Simulation of such systems has been performed using analytical approaches ^{27–30} as well as numerical frameworks. ^{31–34} In analytical studies, beam theory and stress equilibrium equations were used to study uniaxial mode displacement (one-dimensional), ^{18,28} and von Karman theory for the nonlinear large deformations of plates and shells was applied to study complex two-dimensional wrinkling systems. ^{35–40}

On the other hand, in the numerical studies, finite element modelling was utilized to explore deformation instabilities. Such instabilities are inherently complex, and linear elasticity for the constituents is assumed to simplify analysis and reduce computational costs. However, elastomers have viscous time dependent response in addition to elastic behavior. In linear elastic material, since all the energy stored in loading is returned once the load is removed, the rate of strain does not play a role in the response of the system. However, in viscoelastic material, some of the energy dissipates once the load is removed, so strain rate is a determining factor in the system response. Here, we study the use of viscoelastic models to determine nanoscale wrinkle morphology for bilayered material composites, and we relate the results to a recently studied autoregulatory experimental setup that we and others studied using elastic models,1 enabling predictions of viscoelastic bilayer structures that would have improved autoregulatory properties.

In viscoelastic materials, some rate dependent deformation occurs along with the recoverable elastic deformation coexists. As such, a linear combination of springs and dampers (damped mechanical oscillators) is used in lumped modeling of viscoelastic materials.41 The springs are used to represent elastic recoverable behavior, while dampers are used for capturing the rate of dissipative deformation under constant force. Several rheological models have been proposed for modeling the time-dependent stress and strain evolution in polymers. Each model has its own arrangement of springs and dampers, and all of these are modeled by equivalent electrical circuits.⁴¹ These models include generalized Maxwell (GM), generalized Kelvin-Voigt (GK), and Burger (BR) models. GM is made of several Maxwell elements in parallel where each Maxwell element is made up of a damper and a spring connected in series (Figure S1). On the other hand, GK is made up of a damper and spring in parallel and BR is a combination of GM and GK which would be damper and spring in series followed by damper and spring in parallel (Figure S1).

Viscoelastic models are designed to enable prediction of different mechanical deformations. For example, the GM model could capture stress relaxation but it is not suitable for creep studies while GK could describe creep but not stress relaxation. In the GK model, the strain of the parallel branches would be equal upon a deformation such as compression or tension while the sum of the stress of each branch would give the total stress. The GM model would have

equal stress for each constituent while the total strain would be the sum of the strain contributions of each spring and damper. This explains the model's sensitivity to the type of deformation test (such as stress relaxation or creep) in determining accuracy of the prediction. Burger's model is designed to improve predictive capacity relative to GM and GK. However, for complex stress state rather than simple uniaxial tests such as one-dimensional stress relaxation or creep, it may not be straightforward to determine the most accurate viscoelastic mdoel to use. Thus, rigorous studies may be required, accompanied by validation from experiments to gain a reliable prediction.

In recent studies, ^{1,31-34,44,45} the soft layer has usually been modeled as linear elastic material for simplification and preventing convergence issues but at the expense of losing viscous features of the hydrogel. Utilizing more realistic material models would enable a reliable characterization of the bilayer composite systems for a wide range of material properties. Previously, there have been studies of wrinkle formation for hard thin films on soft substrate composites with the assumption that the soft layer is viscoelastic but utilizing different mechanical theories like the theory of lubrication, 46 a shear lag model,⁴⁷ membrane theory,⁴⁸ and energy minimization. 49 Those methods are complex, and some lack the versatility needed for tuning different parameters for system characterization; however in some cases analytical formulas for viscoelastic behavior have been derived which are often used. For example, Huang et al.⁵⁰ used the Kelvin model to determine the critical stress required for wrinkle formation as

$$\sigma_{c} = -\sqrt{\frac{4(1-v)}{3(1-2v)(1-v_{f})}} \frac{h_{f}}{H} \mu_{f} \mu_{R}$$

where $h_{\rm f}$ is thickness, $\mu_{\rm f}$ is the shear modulus, and $v_{\rm f}$ is Poisson's ratio for the skin. H is the thickness, $\mu_{\rm R}$ is the rubbery modulus, and $v_{\rm f}$ is the Poisson's ratio for the substrate. This equation can only be applied to the systems with a thin viscoelastic layer (when thickness of substrate \ll wavelength of wrinkles). Another limiting case arises for elastic materials, where the critical stress depends on the cube root of the ratio of skin to substrate modulus. While this does not immediately apply to viscoelastic materials, it can be used as a guide for using experimental values of the critical stress to determine effective modulus ratios.

We have recently proposed an autoregulatory system for humidity sensing consisting of a nanoscale wrinkle-patterned hydrogel with tunable feedback cycle time scales where the wrinkled pattern senses humidity variation and a plasmonic nanoparticle (PNP) lattice regulates wrinkling through plasmonic heating. In that study, the hydrogel layer was assumed to be a linear elastic material, and this turned out to be a reasonable approximation based on agreement of the wrinkle properties with experiment. Hydrogels can be purely elastic materials, so that their stiffness is not dependent on the rate or magnitude of deformation, 51,52 or they can be viscoelastic, particularly when the cross-linked polyacrylamide (PAA, elastic) is associated with a viscous solution of un-crosslinked PAA. 53 In practical applications, e.g., in biological systems for drug release, or in device applications where the rapid response of an elastic material is undesirable, viscoelasticity is a desired property. In this case, the tissue's loss moduli, say for fat, spinal cord, liver, or brain, are around 20% of their elastic moduli.⁵⁴ Thus, viscoelasticity should be

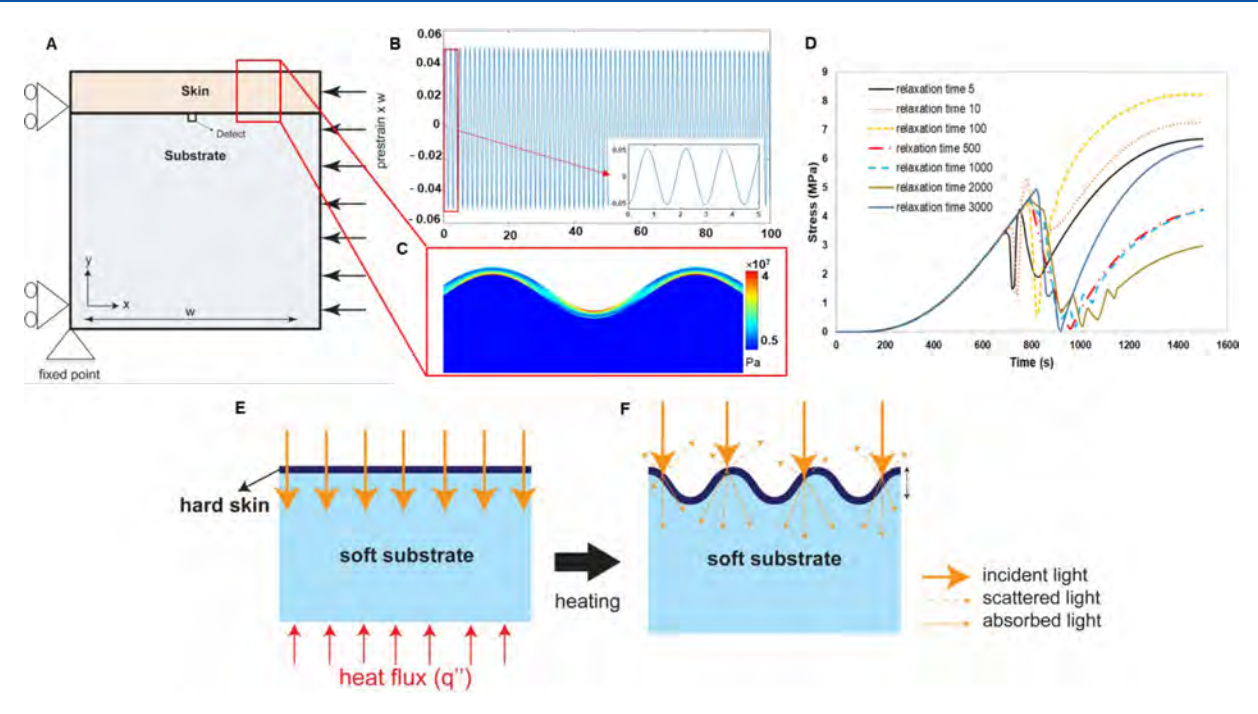


Figure 1. (A) Schematic representation of the bilayered composite including substrate and skin with boundary and initial conditions and defects (defects in the materials properties of the composite layers are essential to produce nanoscale wrinkles. Detailed explanation is in the Method section). This system produces wrinkles by stress applied to one side of the substrate. (B) Generated wrinkles on the surface of the whole composite, where the y-axis represents vertical displacement and x-axis represents position along the strain direction (units in μ m). The inset shows the surface wrinkles for $x = 0-5 \mu$ m. (C) Von Mises stress on a 2 μ m segment of the composite. (D) Time evolution of the stress at a specific point on the interface of skin and substrate around the middle of the sample for different relaxation times (generalized Kelvin model). (E, F) Schematic representation of the system that produce wrinkles by heat generated from light source because of plasmonic heating. (E) Before and (F) after wrinkle generation.

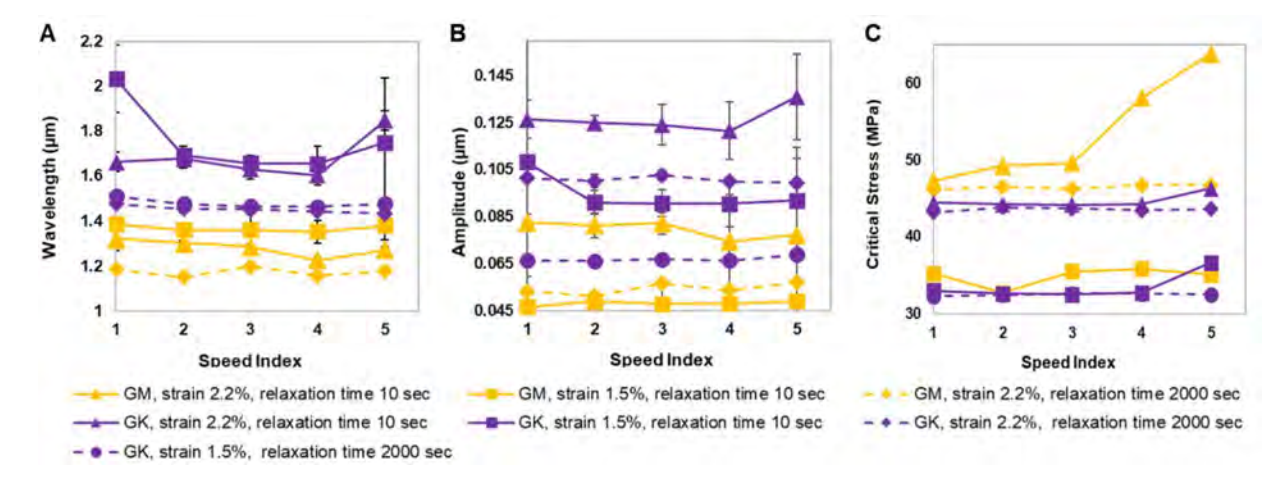


Figure 2. Effect of the strain rate on the morphology of nanoscale wrinkles and the stress distribution at relaxation times of 10 and 2000 s and strain of 1.5% and 2.2% for the GM and GK models of viscoelasticity. Speed index represents strain rate; the higher the index, the faster the strain is applied. The strain speeds are 0.04 (speed index 1), 0.05 (speed index 2), 0.07 (speed index 3), 0.14 (speed index 4), and 0.29 (speed index 5) μ m/s. (A) and (B) represent the average wavelength and amplitude of wrinkles on the surface of the layered composite. (C) represents the critical stress for simulations where wrinkles are generated. The GM model at strain of 1.5% and relaxation time of 2000 s did not produce wrinkles due to low Von Mises stress (data not represented here).

taken into account in real applications, which motivates the present study of nanoscale wrinkle pattern formation.

In this paper, we will explore how viscoelasticity could affect the morphology of nanoscale wrinkle formation using several viscoelastic models. Viscoelastic materials have unique characteristics, and their properties are affected by many factors like strain rate, magnitude of strain, and relaxation time. We will explore the effect of these different factors on the output of wrinkling, with particular attention to the autoregulatory humidity sensor used in our recent work. The findings of this paper would enable design principles in many applications ranging from pressure or humidity sensors to thermal-responsive drug delivery systems.

RESULTS AND DISCUSSION

In our previous study on the autoregulatory composite system with nanoscale wrinkle formation, the system was made up of a hydrogel layer which is PAA with thickness 600 μ m and the thin film on top is polytetrafluoroethylene (50 nm). A time-dependent finite element analysis was performed and validated with experimental data. The simulations were in good agreement with experiments in terms of nanoscale wrinkle dimensions (wavelength and amplitude), time scale, and temperature distribution. In the present study, we simulate the same system with the assumption that the soft layer is viscoelastic. Figure 1A–C,E,F shows details of our structural model, along with an example of the wrinkles that typically form for the models we have considered. Details of the simulations are in the section Method.

Figure 1D illustrates the time evolution of the stress at a specific point in the middle of the specimen at the interface of the skin and substrate, in response to a strain rate of 0.05 μ m/ s, for the GK model. The irregular pattern of the plot indicates a system with geometric nonlinearity. The stress goes up until a certain point as a function of time corresponding to the onset of the wrinkling, and then it drops as the skin stress is significantly relaxed. This happens when the amplitude increases to a size comparable to the thickness of the skin.⁵⁰ Precise details of the drop depend strongly on the relaxation time assumed in the viscoelastic response, with long times corresponding to elastic behavior, where there is a drop to nearly zero stress, followed by a rise due to the assumption that the amplitude continues to grow with time. For short relaxation times (5 and 10 s), we see that the stress can oscillate a couple times, and it never drops as much as in the elastic case before the stress starts rising again.

Effect of Strain Rate and Magnitude on the Wrinkling Morphology. Here we study the dependence of nanoscale wrinkle formation on strain rate, with the strain varying sigmoidally as a function of time (Figure S3). The strain speeds (rate of change of the sigmoidal function) range from 0.04 to 0.29 μ m/s, which we relate to a speed index that varies from 1 to 5, as specified in Figure 2. Both the generalized Maxwell (GM) and generalized Kelvin-Voigt (GK) models for viscoelastic response are considered, and three properties (wavelength, amplitude, and critical stress) are studied. Critical stress is not uniquely defined for viscoelastic models, and it will be strain dependent in general. For this work we have used the highest value of the Von Mises stress at the end of simulations where wrinkling occurs to define the critical stress. Note that this definition likely overestimates the equilibrium critical stress compared to the analytical formula for wrinkling in purely elastic materials.³¹ Our interest here is in studying the variation of critical stress with strain speed, relaxation time, and other parameters, so this lack of precision is of secondary importance. In the Supporting Information, we provide results for another property, minimum stress, in Figures S2, S3, and

According to Figure 2A,B, the GM model gives a smaller wavelength and amplitude than GK. The wavelengths and amplitude of nanowrinkles produced on the surface of the skin might vary, so the reported morphology (wavelength and amplitude) is averaged over all generated nanowrinkles on the surface of skin. The standard deviation of the wrinkles on the surface of the system is calculated to determine uniformity of morphology. GK models at low relaxation time and strain of

2.2% had the least uniformity of morphology in both wavelength and amplitude. The Von Mises stress is highest in regions of the wrinkles which are at the extremes (hills and valleys, Figure 1C). By increasing the rate of applied strain, the critical stress was either almost constant (GK at relaxation time of 2000 s, GM at relaxation time of 10 s and strain of 1.5, and relaxation time of 2000 s and strain of 2.2%) or increasing (GK at relaxation time 10 s and GM at relaxation time 10 and strain 2.2%).

According to Figure 2C, the critical stress is more sensitive to the strain rate at lower relaxation times, and this is true for the nanoscale wrinkle morphologies as well. Also, there was less sensitivity of the morphology to strain rate for higher relaxation times. As the relaxation time increases, the material dissipates less energy following the load which is indicative of linear elasticity. This can be understood in terms of the Deborah number, which combines both elasticity and viscosity of the material. At a lower Deborah number, the material's behavior is more fluid-like with a Newtonian viscous flow representation, while the higher Deborah number indicates the non-Newtonian regime with an elasticity dominant solid-like behavior, and for a linear elastic solid (Hookean elastic solids), the relaxation time is infinite. Thus, at high relaxation times, less sensitivity to the strain rate is expected. Figure 2C shows that the critical stress of GM is higher than for the GK model (at a specific strain and relaxation time) with the exception of the highest strain rate (speed index 5), low relaxation time, and strain 1.5% (Figure 2C and Figure S3). The GM model with a strain of 1.5% and relaxation time of 2000 s did not produce global wrinkles due to having a very low value of the highest Von Mises stress (20 MPa). We attempted to modify the defects (defined in the caption of Figure 1 along with a detailed explanation in the Method section) to discover whether that could produce wrinkles in the GM model. Revising the defects could produce some wrinkles locally around the areas with defects, but the wrinkles were not global

Figure 2A and Figure 2B show that by decreasing the magnitude of strain, the wavelength and amplitude increases and decreases, respectively, with only one exception (for the wavelength: GK model, magnitude of strain 2.2%, relaxation time 10 s). This agrees with the experimental study of Jiang et al.⁵⁵ on single-crystal ribbons of silicon bonded to a prestrained substrate of polydimethylsiloxane. The wavelength increases and amplitude decreases as a result of strain reduction due to a drop in energy of the system, and there is also a decline in the critical stress (Figure 2C).

The wavelength and amplitude vary in the ranges of 0.9–22% and 14–43%, respectively, for both GM and GK models at different relaxation times when the magnitude of strain is reduced from 2.2% to 1.5%. Jiang et al.⁵⁵ found experimentally that when strain dropped from 2.2% to 1.5% the wavelength and amplitude varied 8.6% and 24%, respectively. The systems are different in both the material properties of soft substrates and hard skins in terms of Young moduli and Poisson ratios as well as thickness of the skins and substrates. Further investigation is required to study the sensitivity of the wrinkle's wavelength on the mechanical properties of the composites, in addition to varying the experimental conditions (strain rates and magnitude).

Effect of Relaxation Time on the Wrinkling Morphology. Relaxation time is a characteristic time of the system's relaxation following an external perturbation, as defined by the

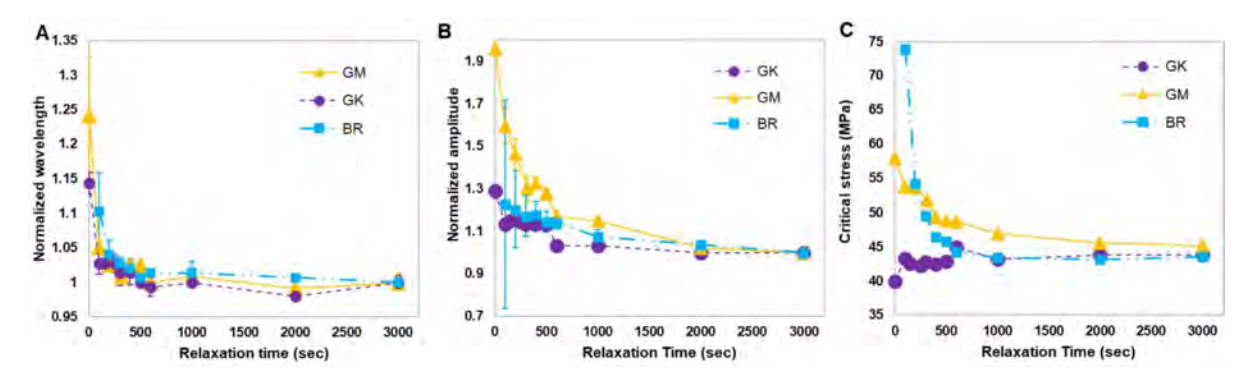


Figure 3. Effect of relaxation time on the wrinkling morphology and stress distribution for the GM, GK, and BR models of viscoelasticity at relaxation times ranging from 5 to 3000 s. (A) and (B) illustrate the average wavelength and amplitude, normalized by their corresponding values at a relaxation time of 3000 s (close to linear elastic). (C) represents the magnitude of the highest stress after the nanowrinkles are generated. The strain for all models is 2.2%.

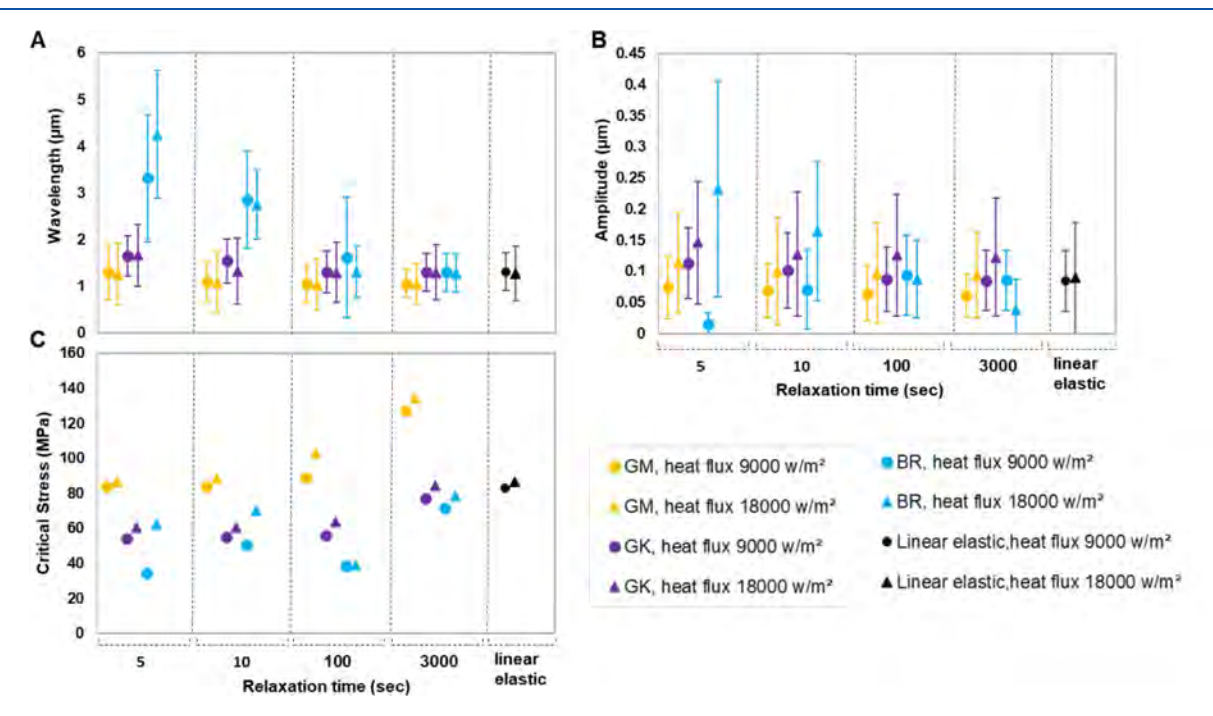


Figure 4. Wrinkling induced in a thermomechanical system using GM, GK, and BR models at heat flux 9000 and 18 000 w/m² and relaxation times 5, 10, 100, 3000 s. (A) and (B) show the average wavelength and amplitude. (C) illustrates the critical stress.

ratio of viscosity to modulus. Tuning the relaxation time with the parameters of the autoregulatory system like strain rate could be important for achieving a desired wrinkling morphology and as a result the time scale of autoregulatory response. These viscoelastic properties of the hydrogel (like relaxation time) can be tuned by adjusting the cross-linker concentration in hydrogel synthesis to make it stiffer or softer. ^{53,56} It should be noted that the change in the cross-linker concentration would alter the equilibrium elastic modulus in addition to the instantaneous elastic modulus of the system. ⁵⁶

Simulations were performed at different relaxation times ranging from very small values (5 s) to high magnitudes (3000 s) (Figure 3). The wavelength and amplitude are normalized by their values at large relaxation times (wavelength 1.16, 1.47, and 1.45 μ m and amplitude 0.047, 0.097, and 0.102 μ m for the GM, GK, and BR models, respectively). For all models, as the relaxation time increases, the wavelength and amplitude decrease, especially at relaxation times below 100 s, until a

plateau is reached (Figure 3A,B) at around 1000 s. This agrees with the experimental work by Das et al.⁵⁷ They tuned the viscoelastic properties of the polydimethylsiloxane (PDMS) polymer by different concentration of cross-linker and found that as the storage modulus (G') increases, the wavelength and amplitude of wrinkles decrease. The morphology of all models converges as the relaxation time increases which indicates that the system becomes less sensitive to the model selection when approaching the linear elasticity limit (Figure 3A,B). The critical stress for the GK, GM, and BR models and a small relaxation time (e.g., 100 s) is around 43, 54, and 74 MPa, respectively (Figure 3C). For the GK model, the critical stress increases with relaxation time, while for GM and BR the critical stress decreases and finally the values converge at very high relaxation times (to around 44 MPa). While there is more fluctuation in the critical stress at lower relaxation times for GM and GK, the BR model's stress drops rapidly as relaxation time increases (from 74 to 54 MPa for relaxation times 100 and 200 s, respectively).

Based on elastic theory that was mentioned in the Introduction, the smaller is the ratio of the elastic moduli (substrate to skin), the bigger are the wavelengths. The results in Figure 3C indicate that the GM model has a lower effective modulus ratio, as the critical stress is higher, and this results in the generation of larger wrinkles (bigger periods of oscillation) and larger amplitudes. This is true for both the GM and BR models compared to the GK model. In the GK model, there is a parallel configuration of series and dampers, so each branch has less stress compared to the GM model which has the spring and damper in series. As a result, the GK model behaves more like the linear elastic case and variation of the critical stress in the GK model is not as large as in the GM model as the relaxation time increases. For very large relaxation times, the system is closer to linear elasticity, so the morphology of all models and critical stress converge.

Effect of Heat Flux and Viscoelastic Properties on the Wrinkling Induced in the Thermomechanical System. In autoregulatory systems, a driving force is required to manipulate the wrinkling in a cyclic manner. An example of such an autoregulatory system with the capability of programming time scale of the regulatory cycle is presented in our recent paper. In response to the moisture, the nanoscale wrinkled layer flattens which allows light to reach the bottom of the composite where there is a plasmonic nanoparticle lattice. Light absorption by the nanoparticle lattice generates plasmonic heating which dries out the hydrogel, and nanowrinkles are formed. Once the wrinkles form, more light is scattered and less is absorbed by the hydrogel, so the temperature goes down and humidity increases in the system, resulting in the wrinkles that flatten. This cyclic manner repeats again and again. In this section a system which couples both mechanical and thermal dynamical behavior with the assumption of viscoelastic material is discussed using the GM, GK, and BR models (Figure 1E,F).

The morphology of nanoscale wrinkles is presented in Figure 4 for relaxation times ranging from 5 to 3000 s and heat flux of 9000 and 18 000 w/m² after 450 and 180 s, respectively. While the magnitude of heat flux affected the time scale of wrinkle formation, the morphology of the system was less sensitive to temperature and thus to the heat flux for the GK and GM models compared with BR model (wavelength and amplitude at high and low relaxation times in Figure 4A,B). The lack of sensitivity of morphology to heat flux agrees with our experimental measurements. A lower heat flux produced nanowrinkles at lower surface temperature (around 56 °C for all relaxation times, Figure S8). Thus, less surface stress was generated (Figure 4C) and it took longer for nanowrinkles to form (450 and 180 s for heat flux of 9000 and 18 000 w/m², respectively). Like the mechanically perturbed system, the wavelength of the wrinkles decreases as the relaxation time increases, and this drop is highest with the BR model. (For heat flux 9000 w/m 2 (18 000) there is a 23.78% (20%), 26.53% (28.48%), and 153.43% (232.96%) drop in the wavelength of GM, GK, and BR, respectively, when relaxation time is increased from 5 to 3000 s.) While there is more fluctuation in the amplitude predicted by the BR model, a 19-32% drop in the GM and GK models is observed by increasing the relaxation times.

The morphology of the nanoscale wrinkles for a linear elastic model of the same system is also presented in Figure 4A,B. By increasing the relaxation time, the morphology approaches the corresponding linear elastic system. As the hydrogel approaches a linear elastic material, the wrinkles would have a more uniform wavelength (standard deviation decreases). However, this not the case for the amplitude, where there is substantial variation in the results for different choices of viscoelastic behavior. In general, a higher heat flux (18 000 w/ $\rm m^2$) generates less uniform amplitude (with an exception: BR model at relaxation time 3000 s).

Figure 4C shows that the critical stress is increased by increasing the relaxation time at higher relaxation and is almost constant at lower relaxation times except for the BR model. There is no significant difference in the critical stress generated at higher versus lower temperatures. This might differ based on the evolution of nanoscale wrinkles which is discussed in other publications. The viscoelasticity effect would be more prominent in polymers above the glass transition temperature. However, a molecular level study of such behavior is required to capture the effect of viscoelasticity under these circumstances.

GK Model Is the Best Predictor for Both Mechanical and Thermomechanical Wrinkling Bilayer Hydrogel System. The accuracy of each viscoelasticity model is mainly dependent on the type of deformation the material is experiencing and on the mechanical properties of the system. We attempted to understand which model of viscoelasticity is the best predictor of the hydrogel system developed in our earlier study. Figure 5 presents the evolution of the nanoscale

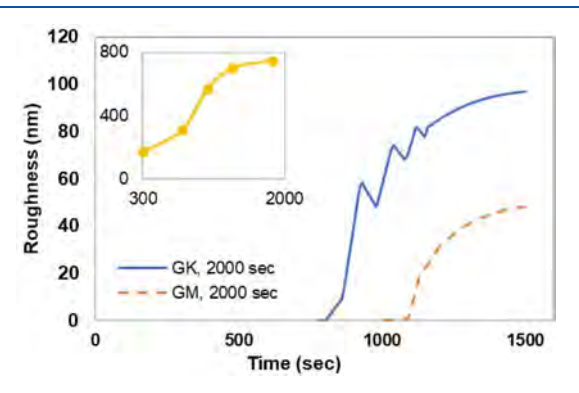


Figure 5. Time evolution of root-mean-square (roughness) of the nanowrinkles for GM (dashed line) and GK (solid line) models at relaxation time 2000 s. The inset shows experimental time evolution of the roughness for a linear elastic substrate (reproduced from our recent work 1). The inset has the same units as in the main figure.

wrinkle roughness for GM and GK at relaxation times of 2000 s following uniaxial compressive strain. The GK model for all relaxation times illustrates three phases of the growth: initial slow growth followed by a rapid increase in the middle phase (with oscillations due to mechanical instabilities similar to Figure 1D) and finally reaching a plateau in the third phase. This is true for different relaxation times (5, 100, 2000 s, Figure S9). A similar pattern was observed in our experimental data for this system (see inset of Figure 5). Since the experiments were based on a linear elastic hydrogel (numerical simulation with the linear elasticity could qualitatively and quantitatively predict the morphology of wrinkles and time scale of wrinkling), the GM and GK models for high relaxation times (2000 s) that are close to linear elasticity should be comparable to the experimental observations. As such, although the second and third phases are present in the GM model results for a relaxation time of 2000 s, the initial slow

growth phase of the wrinkles is absent in the GM model while the GK model properly includes all three phases. These three phases of growth are also reported in other experimental⁵⁸ and theoretical research.^{46,50} Furthermore, in the thermomechanical system described earlier, the morphology of wrinkles predicted by the GK model was the most accurate when compared at a relaxation time 3000 s with the validated linear elastic model (Table 1). Comparison with the BR model (not presented) is less accurate than for GK, as demonstrated in Figure 4A,B.

Table 1. Variation of Wavelengthand Amplitude at Relaxation Time 3000 s of Thermomechanical System from Linear Elastic Model for GK and GM Models

% variation from linear elastic	wavelength (amplitude) heat flux (w/m²)	
	9000	18000
GK	-0.76 (0.35)	1.5 (6.2)
GM	-19.6 (-27.2)	-17.9 (-18.3)

Optical Transmission Spectrum of Inhomogeneous Thin Films Is Significantly Influenced by Surface Morphology. We showed that for the GK model the amplitude of the system is altered up to 30% for different relaxation times. Since nanoscale wrinkle formation and then disappearance are crucial to the autoregulatory response of the system, in this section we will discuss how morphology would affect the transmission of light (Figure 1E,F). Plus, by modulating the optical properties, an optimum material for the substrate and skin could be selected to customize the autoregulatory response (e.g., time scale) of the system for the specific application.

Swanepoel derived an analytical expression in which the transmission spectrum could be used to calculate the optical constants of an inhomogeneous thin film. We have used this expression to study the effect of thickness, refractive index, and surface roughness on the transmission spectrum (description of the model in the Supporting Information). Figure 6 shows the light transmission across the skin and substrate as a function of the wrinkling amplitude in an inhomogeneous nanoscale wrinkled surface at different wavelengths ranging from 500 to 900 nm. According to the plot and depending on the refractive indices of the skin and substrate, we can have as large as 10% of variation (light wavelength of 500 nm in Figure

6A) or even larger in the transmission of light by variation in amplitude. This indicates the significance of morphology on the amount of light reaching the plasmonic nanoparticle arrays and subsequent heat generated because of plasmonic heating. Thus, as we showed in the previous section, it will then affect the time scale of the heat transfer and subsequent autoregulatory response of the system. This is critical as the main drawback of the current autoregulatory systems is lack of flexibility to program their regulatory feedback loop for a wide range of time scales.

CONCLUSION

We have demonstrated a framework for numerical simulation of nanoscale wrinkle formation in a bilayer hydrogel system with mechanical and thermal perturbation of the hydrogel described using a wide range of viscoelastic parameters (GM, GK, and BR models) which govern response of the system to uniaxial strain or heat flux. The model is validated with experimental data that closely match a linear elastic composite system at very high relaxation times. We find that manipulation of the strain rate and magnitude affects the morphology of wrinkles, with the wavelength and amplitude varying up to 24% and 85%, respectively, as relaxation time is varied. Hence, the morphology of nanowrinkles can be programmed by tuning the relaxation time of the wrinkles. The time evolution of the system as well as comparison with the validated linear elastic model and experimental data demonstrated that the GK model is the best predictor in both mechanical and thermomechanical systems. Finally, we demonstrated that the light transmission could be adjusted by the morphology of nanowrinkles. This is obtained by selecting the correct combination of refractive indices for the skin and substrate. The findings of this paper will help to facilitate programmability of the next generation of autoregulatory systems and responsive materials. For example, nanoscale wrinkle formation due to uniaxial strain could be integrated with a pressure sensor, and thermal actuation of the system could be associated with thermal-responsive drug delivery systems.

METHOD

Computational Simulations. Our system, which is based on an elastic model that we previously studied, 1 is made up of substrate and skin. The substrate has a thickness of 600 μ m and width of 100 μ m. The skin thickness is 50 nm. As in the earlier elastic modeling, a roller boundary condition is set on the left side of the system so that the surface touching the roller is free to go up and down while not

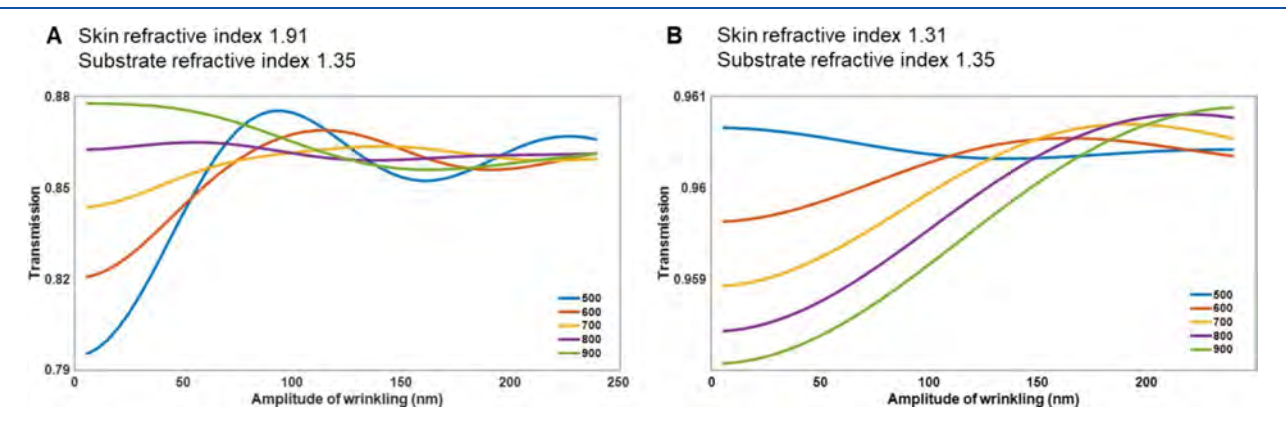


Figure 6. Light transmission across the skin and substrate for different wavelengths (500, 600, 700, 800, 900 nm) as a function of wrinkling amplitude in an inhomogeneous wrinkled surface. Choices of refractive index for skin and substrate are (A) 1.91 and 1.35 and (B) 1.31 and 1.35.

allowed to move left and right (Figure 1A). As a result, there is a symmetry in geometry, material properties, and boundary conditions such that a model 100 μ m long is equivalent to a model 200 μ m length, making the model computationally less costly.

Viscoelasticity in this work was comprised of viscous and elastic components which could be arranged in series or parallel configurations. Relaxation time, shear modulus, Young modulus, as well as Poisson ratio were used to specify the system. Multiple relaxation times ranging from 5 to 3000 s were used in our analysis. The generalized Maxwell (GM) model is comprised of the spring and damper in series, while in the generalized Kelvin–Voigt (GK) the spring and damper are in parallel. Burger's (BR) model has a combination of GM and GK branches in series. We assumed the BR model's relaxation times in the GM and GK branches are the same.

The amplitude and wavelength of wrinkles were normalized using the values at very high relaxation times (by increasing the relaxation time, the material tends to more linear elastic behavior). Critical stress is the highest value of the von Mises stress measured on the wrinkles' surface at the end of those simulations that produce wrinkles. A smooth step function was used to apply the strain as a perturbation to the model. To explore the sensitivity of the viscoelastic polymer on the perturbation rate, the transition zone of the step function was altered to manipulate the strain rate (Figure S3). The strain speeds are 0.04 (speed index 1), 0.05 (speed index 2), 0.07 (speed index 3), 0.14 (speed index 4), and 0.29 (speed index 5) μ m/s.

The Young moduli of the substrate and skin were 4 and 1200 MPa, respectively. The Poisson ratios of both were 0.46. The skin is assumed to be linear elastic, while the substrate is viscoelastic. To introduce defects in the mesh (see additional discussion below), some of the finite elements at the interface of the substrate and skin in the substrate region were selected to make their material properties to be the same as skin. ^{31–33}

A finite element analysis is performed to model the highly nonlinear equilibrium equation of the wrinkle formation. Comsol Multiphysics is used for this modeling. The time step is set to be 1, 2, and 10 s for relaxation times of 5, 10, and larger than 10 s, respectively. A gradient element size in the skin and substrate is designed that increases gradually from top to the bottom. Skin mesh size ranges from 0.001 μ m to 0.02 μ m and from 0.18 μ m to 40.2 μ m in the skin and substrate, respectively.

Thermomechanical finite element analysis of the system is explained in detail in our publication by Lee et al. Briefly, a plasmonic heat flux at the bottom of the system is applied to have high (18000 w/m²) and low temperature (9000 w/m²) at the surface of wrinkles. The free surfaces of the system have convection with the convection coefficient of $h=15^{\rm w}/\rm m^2\rm k$ and temperature 25 °C. The schematic figure illustrates boundary conditions (Figure S10). Properties of the skin and substrate are listed in the Table 2. The Supporting Information provides more details on the governing equations of viscoelastic models.

Table 2. Materials Properties of Substrate and Skin

	specific heat capacity (J/(kg °C))	thermal expansion coefficient (1/K)	thermal conductivity (W/(m·K))	density (kg/m³)
substrate	1555.71	-1.5×10^{-6}	0.05	1130 1780
skin	1500	3×10^{-4}	0.25	

Defects are inherent characteristics of materials. Heterogeneity in microstructure and the mechanical response of materials are the source of buckling and wrinkling following internal or external perturbations. So a numerical solution of the models requires having some type of instability to produce bifurcation and wrinkling in the systems we are studying. ^{31,34} To impose these instabilities, several methods have been presented in the literature. One method is adding the heterogeneity by making a gradient to the Young's modulus and Poisson's ratio along the direction perpendicular to the substrate. ^{44,45} Saha ³⁴ included a wavy mesh imperfection through sinusoidal

displacement of the mesh in the skin boundary. Adding a mesh imperfection by imposing roughness in the skin surface is another method to incorporate imperfection in the model.⁶⁰ All of these defects are complex, based on trial and error, require prior preparation, and the fixing of free variables as well as interpretation and validation. Nikravesh et al.^{31–33} used a straightforward and computationally efficient approach by incorporating imperfections through adding heterogeneity in the material properties of the substrate at the interface of the substrate and skin.

ASSOCIATED CONTENT

Supporting Information

The Supporting Information is available free of charge at https://pubs.acs.org/doi/10.1021/acsanm.2c03412.

(1) Summary of the models of viscoelasticity used in this work; (2) theory of light transmission from inhomogeneous thin films; (3) figure showing sigmoid function used to tune strain; (4 to 6) several figures showing minimum strain results of the effect of strain rate, effect of relaxation time and thermomechanical modeling, respectively; (7) figure showing local wrinkles that arise when displacements fail to generate global wrinkles; (8) time evolution of the roughness of the wrinkles for the three viscoelastic models at different relaxation times; (9) figure showing bilayer model used to include plasmonic heating (PDF)

AUTHOR INFORMATION

Corresponding Author

George C. Schatz — Department of Chemical and Biological Engineering, Northwestern University, Evanston, Illinois 60208, United States; Department of Chemistry, Northwestern University, Evanston, Illinois 60208, United States; orcid.org/0000-0001-5837-4740; Email: g-schatz@northwestern.edu

Author

Zeynab Mousavikhamene – Department of Chemical and Biological Engineering, Northwestern University, Evanston, Illinois 60208, United States

Complete contact information is available at: https://pubs.acs.org/10.1021/acsanm.2c03412

Notes

The authors declare no competing financial interest.

ACKNOWLEDGMENTS

This work was supported by the National Science Foundation (NSF RAISE CMMI-1848613). We thank Young-Ah Lucy Lee and Teri W. Odom for comments.

■ REFERENCES

- (1) Lee, Y. A. L.; Mousavikhamene, Z.; Amrithanath, A. K.; Neidhart, S. M.; Krishnaswamy, S.; Schatz, G. C.; Odom, T. W. Programmable Self-Regulation with Wrinkled Hydrogels and Plasmonic Nanoparticle Lattices. *Small* **2022**, *18*, 2103865.
- (2) Lacour, S. P.; Wagner, S.; Huang, Z.; Suo, Z. Stretchable gold conductors on elastomeric substrates. *Applied physics letters* **2003**, 82 (15), 2404–2406.
- (3) Lee, W.-K.; Kang, J.; Chen, K.-S.; Engel, C. J.; Jung, W.-B.; Rhee, D.; Hersam, M. C.; Odom, T. W. Multiscale, hierarchical patterning of graphene by conformal wrinkling. *Nano Lett.* **2016**, *16* (11), 7121–7127.

- (4) Linke, P.; Suzuki, R.; Yamamoto, A.; Nakahata, M.; Kengaku, M.; Fujiwara, T.; Ohzono, T.; Tanaka, M. Dynamic contact guidance of myoblasts by feature size and reversible switching of substrate topography: orchestration of cell shape, orientation, and nematic ordering of actin cytoskeletons. *Langmuir* **2019**, *35* (23), 7538–7551.
- (5) Jiang, X.; Takayama, S.; Qian, X.; Ostuni, E.; Wu, H.; Bowden, N.; LeDuc, P.; Ingber, D. E.; Whitesides, G. M. Controlling mammalian cell spreading and cytoskeletal arrangement with conveniently fabricated continuous wavy features on poly (dimethylsiloxane). *Langmuir* **2002**, *18* (8), 3273–3280.
- (6) Chen, C. S.; Mrksich, M.; Huang, S.; Whitesides, G. M.; Ingber, D. E. Geometric control of cell life and death. *Science* **1997**, *276* (5317), 1425–1428.
- (7) Roy, S.; Bhandaru, N.; Das, R.; Harikrishnan, G.; Mukherjee, R. Thermally tailored gradient topography surface on elastomeric thin films. ACS Appl. Mater. Interfaces 2014, 6 (9), 6579–6588.
- (8) Miao, L.; Wan, J.; Song, Y.; Guo, H.; Chen, H.; Cheng, X.; Zhang, H. Skin-inspired humidity and pressure sensor with a wrinkle-on-sponge structure. *ACS Appl. Mater. Interfaces* **2019**, *11* (42), 39219–39227.
- (9) Jung, W.-B.; Cho, S.-Y.; Yun, G.-T.; Choi, J.; Kim, Y.; Kim, M.; Kang, H.; Jung, H.-T. Hierarchical metal oxide wrinkles as responsive chemical sensors. *ACS Applied Nano Materials* **2019**, 2 (9), 5520–5526.
- (10) Kim, P.; Hu, Y.; Alvarenga, J.; Kolle, M.; Suo, Z.; Aizenberg, J. Rational design of mechano-responsive optical materials by fine tuning the evolution of strain-dependent wrinkling patterns. *Advanced Optical Materials* **2013**, *1* (5), 381–388.
- (11) Ohzono, T.; Suzuki, K.; Yamaguchi, T.; Fukuda, N. Optical Diffusion: Tunable Optical Diffuser Based on Deformable Wrinkles (Advanced Optical Materials 5/2013). *Advanced Optical Materials* **2013**, *1* (5), 352–352.
- (12) Lee, W.-K.; Engel, C. J.; Huntington, M. D.; Hu, J.; Odom, T. W. Controlled three-dimensional hierarchical structuring by memory-based, sequential wrinkling. *Nano Lett.* **2015**, *15* (8), 5624–5629.
- (13) Lee, W.-K.; Jung, W.-B.; Nagel, S. R.; Odom, T. W. Stretchable superhydrophobicity from monolithic, three-dimensional hierarchical wrinkles. *Nano Lett.* **2016**, *16* (6), 3774–3779.
- (14) Giordano, M. C.; Sacco, F. d.; Barelli, M.; Portale, G.; Buatier de Mongeot, F. Self-Organized Tailoring of Faceted Glass Nanowrinkles for Organic Nanoelectronics. *ACS Applied Nano Materials* **2021**, *4* (2), 1940–1950.
- (15) Huntington, M. D.; Engel, C. J.; Odom, T. W. Controlling the orientation of nanowrinkles and nanofolds by patterning strain in a thin skin layer on a polymer substrate. *Angew. Chem.* **2014**, *126* (31), 8255–8250
- (16) Panse, K. S.; Zhou, S.; Zhang, Y. 3D Mapping of the Structural Transitions in Wrinkled 2D Membranes: Implications for Reconfigurable Electronics, Memristors, and Bioelectronic Interfaces. ACS Applied Nano Materials 2019, 2 (9), 5779–5786.
- (17) Breid, D.; Crosby, A. J. Surface wrinkling behavior of finite circular plates. *Soft Matter* **2009**, *5* (2), 425–431.
- (18) Chung, J. Y.; Nolte, A. J.; Stafford, C. M. Surface wrinkling: a versatile platform for measuring thin-film properties. *Advanced materials* **2011**, 23 (3), 349–368.
- (19) Chen, Z.; Zhang, X.; Song, J. Surface wrinkling of an elastic graded layer. Soft Matter 2018, 14 (43), 8717–8723.
- (20) Ryu, D.; Mongare, A. Corrugated photoactive thin films for flexible strain sensor. *Materials* **2018**, *11* (10), 1970.
- (21) Khang, D. Y.; Rogers, J. A.; Lee, H. H. Mechanical buckling: mechanics, metrology, and stretchable electronics. *Adv. Funct. Mater.* **2009**, *19* (10), 1526–1536.
- (22) Peterson, R.; Hobart, K.; Kub, F.; Yin, H.; Sturm, J. Reduced buckling in one dimension versus two dimensions of a compressively strained film on a compliant substrate. *Applied physics letters* **2006**, 88 (20), 201913.
- (23) Cutolo, A.; Pagliarulo, V.; Merola, F.; Coppola, S.; Ferraro, P.; Fraldi, M. Wrinkling prediction, formation and evolution in thin films

- adhering on polymeric substrata. Materials & Design 2020, 187, 108314.
- (24) Hsueh, H.-Y.; Chen, M.-S.; Liaw, C.-Y.; Chen, Y.-C.; Crosby, A. J. Macroscopic geometry-dominated orientation of symmetric microwrinkle patterns. ACS Appl. Mater. Interfaces 2019, 11 (26), 23741–23749
- (25) Yang, S.; Khare, K.; Lin, P. C. Harnessing surface wrinkle patterns in soft matter. *Adv. Funct. Mater.* **2010**, 20 (16), 2550–2564.
- (26) Ohzono, T.; Shimomura, M. Ordering of microwrinkle patterns by compressive strain. *Phys. Rev. B* **2004**, *69* (13), 132202.
- (27) Allen, H. G. Analysis and Design of Structural Sandwich Panels: The Commonwealth and International Library: Structures and Solid Body Mechanics Division; Pergamon, 1969; p 283.
- (28) Holland, M.; Li, B.; Feng, X.; Kuhl, E. Instabilities of soft films on compliant substrates. *Journal of the Mechanics and Physics of Solids* **2017**. 98, 350–365.
- (29) Volynskii, A.; Bazhenov, S.; Lebedeva, O.; Bakeev, N. Mechanical buckling instability of thin coatings deposited on soft polymer substrates. *J. Mater. Sci.* **2000**, 35 (3), 547–554.
- (30) Jackson, K.; Allwood, J. The mechanics of incremental sheet forming. *Journal of materials processing technology* **2009**, 209 (3), 1158–1174.
- (31) Nikravesh, S.; Ryu, D.; Shen, Y.-L. Direct numerical simulation of buckling instability of thin films on a compliant substrate. *Adv. Mech. Eng.* **2019**, *11* (4), 1–15.
- (32) Nikravesh, S.; Ryu, D.; Shen, Y.-L. Instabilities of thin films on a compliant Substrate: Direct numerical Simulations from Surface Wrinkling to Global Buckling. *Sci. Rep.* **2020**, *10* (1), 5728.
- (33) Nikravesh, S.; Ryu, D.; Shen, Y.-L. Instability driven surface patterns: Insights from direct three-dimensional finite element simulations. *Extreme Mechanics Letters* **2020**, *39*, 100779.
- (34) Saha, S. K. Predictive design and fabrication of complex micro and nano patterns via wrinkling for scalable and affordable manufacturing. Ph.D. Thesis, Massachusetts Institute of Technology, 2014.
- (35) Song, J.; Jiang, H.; Choi, W.; Khang, D.; Huang, Y.; Rogers, J. An analytical study of two-dimensional buckling of thin films on compliant substrates. *J. Appl. Phys.* **2008**, *103* (1), 014303.
- (36) Huang, Z.; Hong, W.; Suo, Z. Nonlinear analyses of wrinkles in a film bonded to a compliant substrate. *Journal of the Mechanics and Physics of Solids* **2005**, *53* (9), 2101–2118.
- (37) Chen, X.; Hutchinson, J. W. Herringbone buckling patterns of compressed thin films on compliant substrates. *J. Appl. Mech.* **2004**, *71* (5), 597–603.
- (38) Audoly, B.; Boudaoud, A. Buckling of a stiff film bound to a compliant substrate—Part I:: Formulation, linear stability of cylindrical patterns, secondary bifurcations. *Journal of the Mechanics and Physics of Solids* **2008**, *56* (7), 2401–2421.
- (39) Uchida, N. Orientational order in buckling elastic membranes. *Physica D: Nonlinear Phenomena* **2005**, 205 (1–4), 267–274.
- (40) Uchida, N.; Ohzono, T. Orientational ordering of buckling-induced microwrinkles on soft substrates. *Soft Matter* **2010**, *6* (22), 5729–5735.
- (41) Morro, A. Modelling of viscoelastic materials and creep behaviour. *Meccanica* **2017**, *52* (13), 3015–3021.
- (42) Hang, J.-T.; Kang, Y.; Xu, G.-K.; Gao, H. A hierarchical cellular structural model to unravel the universal power-law rheological behavior of living cells. *Nat. Commun.* **2021**, *12* (1), 6067.
- (43) Berret, J.-F. Local viscoelasticity of living cells measured by rotational magnetic spectroscopy. *Nat. Commun.* **2016**, 7 (1), 10134.
- (44) Chapman, C. T.; Paci, J. T.; Lee, W.-K.; Engel, C. J.; Odom, T. W.; Schatz, G. C. Interfacial effects on nanoscale wrinkling in gold-covered polystyrene. ACS Appl. Mater. Interfaces 2016, 8 (37), 24339–24344.
- (45) Paci, J. T.; Chapman, C. T.; Lee, W.-K.; Odom, T. W.; Schatz, G. C. Wrinkles in polytetrafluoroethylene on polystyrene: persistence lengths and the effect of nanoinclusions. *ACS Appl. Mater. Interfaces* **2017**, *9* (10), 9079–9088.

- (46) Im, S.; Huang, R. Evolution of wrinkles in elastic-viscoelastic bilayer thin films. *Journal of Applied Mechanics* **2005**, *72*, 955–961.
- (47) Huang, R.; Suo, Z. Wrinkling of a compressed elastic film on a viscous layer. *J. Appl. Phys.* **2002**, *91* (3), 1135–1142.
- (48) Lee, E.-S.; Youn, S.-K. Finite element analysis of wrinkling membrane structures with large deformations. *Finite Elements in Analysis and Design* **2006**, 42 (8–9), 780–791.
- (49) Im, S. H.; Huang, R. Wrinkle patterns of anisotropic crystal films on viscoelastic substrates. *Journal of the Mechanics and Physics of Solids* **2008**, *56* (12), 3315–3330.
- (50) Huang, R.; Im, S. H. Dynamics of wrinkle growth and coarsening in stressed thin films. *Phys. Rev. E* 2006, 74 (2), 026214.
- (51) Engler, A.; Bacakova, L.; Newman, C.; Hategan, A.; Griffin, M.; Discher, D. Substrate compliance versus ligand density in cell on gel responses. *Biophysical journal* **2004**, *86* (1), 617–628.
- (52) Engler, A. J.; Sen, S.; Sweeney, H. L.; Discher, D. E. Matrix elasticity directs stem cell lineage specification. *Cell* **2006**, *126* (4), 677–689.
- (53) Charrier, E. E.; Pogoda, K.; Li, R.; Park, C. Y.; Fredberg, J. J.; Janmey, P. A. A novel method to make viscoelastic polyacrylamide gels for cell culture and traction force microscopy. *APL Bioeng* **2020**, *4* (3), 036104–036104.
- (54) Charrier, E. E.; Pogoda, K.; Wells, R. G.; Janmey, P. A. Control of cell morphology and differentiation by substrates with independently tunable elasticity and viscous dissipation. *Nat. Commun.* **2018**, *9* (1), 449.
- (55) Jiang, H.; Khang, D.-Y.; Song, J.; Sun, Y.; Huang, Y.; Rogers, J. A. Finite deformation mechanics in buckled thin films on compliant supports. *Proc. Natl. Acad. Sci. U. S. A.* **2007**, *104* (40), 15607–15612.
- (56) Cacopardo, L.; Guazzelli, N.; Nossa, R.; Mattei, G.; Ahluwalia, A. Engineering hydrogel viscoelasticity. *Journal of the mechanical behavior of biomedical materials* **2019**, 89, 162–167.
- (57) Das, A.; Banerji, A.; Mukherjee, R. Programming feature size in the thermal wrinkling of metal polymer bilayer by modulating substrate viscoelasticity. *ACS Appl. Mater. Interfaces* **2017**, 9 (27), 23255–23262.
- (58) Yoo, P. J.; Lee, H. H. Evolution of a stress-driven pattern in thin bilayer films: Spinodal wrinkling. *Phys. Rev. Lett.* **2003**, *91* (15), 154502
- (59) Swanepoel, R. Determination of surface roughness and optical constants of inhomogeneous amorphous silicon films. *Journal of Physics E: Scientific Instruments* **1984**, *17* (10), 896.
- (60) Zheng, X.-P.; Cao, Y.-P.; Li, B.; Feng, X.-Q.; Yu, S.-W. Surface wrinkling of nanostructured thin films on a compliant substrate. *Comput. Mater. Sci.* **2010**, 49 (4), 767–772.

☐ Recommended by ACS

Friction Dynamics of Hydrogel Substrates with a Fractal Surface: Effects of Thickness

Koki Shinomiya, Yoshimune Nonomura, et al.

JUNE 30, 2020 ACS OMEGA

RFAD 🗹

Surface Effect on Frictional Properties for Thin Hydrogel Films of Poly(vinyl ether)

Nozomi Itagaki, Keiji Tanaka, et al.

DECEMBER 04, 2019 MACROMOLECULES

READ 🗹

Toward Quantitative Prediction of the Mechanical Properties of Tandem Modular Elastomeric Protein-Based Hydrogels

Linglan Fu and Hongbin Li

JUNE 01, 2020 MACROMOLECULES

READ 🗹

Revisiting the Origins of the Fracture Energy of Tough Double-Network Hydrogels with Quantitative Mechanochemical Characterization of the Damage Zone

Takahiro Matsuda, Jian Ping Gong, et al.

NOVEMBER 01, 2021

MACROMOLECULES

READ 🗹

Get More Suggestions >